Appl. Phys. B 92, 439–449 (2008)
DOI: 10.1007/s00340-008-3128-x

Applied Physics B
Lasers and Optics

E. KERSTEL[1,✉]
L. GIANFRANI[2]

Advances in laser-based isotope ratio measurements: selected applications

[1] Centre for Isotope Research, University of Groningen, Nijenborgh 4, 9747AG, Groningen, The Netherlands
[2] Dipartimento di Scienze Ambientali, Seconda Università di Napoli, Via Vivaldi 43, 81100 Caserta, Italy

Received: 1 February 2008/Revised version: 23 May 2008
Published online: 9 August 2008 • © The Author(s) 2008

ABSTRACT Small molecules exhibit characteristic ro-vibrational transitions in the near- and mid-infrared spectral regions, which are strongly influenced by isotopic substitution. This gift of nature has made it possible to use laser spectroscopy for the accurate analysis of the isotopic composition of gaseous samples. Nowadays, laser spectroscopy is clearly recognized as a valid alternative to isotope ratio mass spectrometry. Laser-based instruments are leaving the research laboratory stage and are being used by a growing number of isotope researchers for significant advances in their own field of research. In this review article, we discuss the current status and new frontiers of research on high-sensitivity and high-precision laser spectroscopy for isotope ratio analyses. Although many of our comments will be generally applicable to laser isotope ratio analyses in molecules of environmental importance, this paper concerns itself primarily with water and carbon dioxide, two molecules that were studied extensively in our respective laboratories. A complete coverage of the field is practically not feasible in the space constraints of this issue, and in any case doomed to fail, considering the large body of work that has appeared ever since the review by Kerstel in 2004 (*Handbook of Stable Isotope Analytical Techniques*, Chapt. 34, pp. 759–787).

PACS 07.57.-c; 42.55.Px; 42.62.Fi; 93.90.+y; 91.67.Rx; 92.60.H-; 91.40.Zz; 91.62.Xy

1 Introduction

The accurate measurement of isotope abundance ratios is an extremely important and, in fact, often an indispensable research tool in a wide variety of natural sciences, such as bio-medicine, hydrology, palaeoclimatology and atmospheric physics. The natural variation of isotope ratios, due to chemical reactions and physical processes such as condensation and evaporation, can effectively be used to identify and even quantify sources and sinks in, e.g., the global hydrological and carbon cycles (by virtue of providing an extra mass-balance equation for the rare isotope). Moreover, such variations often yield information on the history of the substance, such as the temperature dependent evaporation and condensation history of atmospheric moisture. Isotopically substituted molecules (isotopologues) can also act as virtually ideal tracers.

Isotope ratio mass spectrometry (IRMS) is the conventional method for measuring isotope ratios and has benefited from over 40 years of research and development. Nowadays IRMS instrumentation is commercially available that reaches a high throughput (several minutes' analysis time per sample) and impressively high levels of precision, typically better than 0.1‰ for $^{18}O/^{16}O$ and $^{13}C/^{12}C$, and 0.5‰ for $^{2}H/^{1}H$ (see, e.g., [2, 3]).[1] Unfortunately, IRMS is incompatible with a condensable gas or a sticky molecule such as water. Therefore, in general, chemical preparation of the sample is required to transfer the water isotope ratio of interest to a molecule that is more easily analyzed. Several techniques, most still commonly used, exist, each with its specific properties, advantages, and shortcomings (see, e.g., [4]). It may be clear that for the larger part the required chemical conversion steps are time-consuming, and often compromise the overall accuracy and throughput [1–6]. Apart from these drawbacks specific to water, IRMS instrumentation is expensive, voluminous and heavy, confined to a laboratory setting, and usually requires a skilled operator. All or most of these issues may be addressed by optical measurement techniques.

In this paper we present an overview of the state-of-the-art, and selected applications, in infrared spectroscopic methods for measuring the stable isotope ratios of water and carbon dioxide as alternatives to isotope ratio mass spectrometry (IRMS).

2 Infrared spectrometry

The gas phase, near and mid-infrared absorption spectra of most small molecules that are of environmental interest show a large number of highly characteristic rotational-vibrational transitions that are very sensitive to isotopic substitution. At sufficiently low vapor pressure and high instrumental resolution the individual ro-vibrational transitions are easily resolved, and can be uniquely assigned to a particular isotopologue. Since the intensity of the experimentally recorded spectral features (whether individually resolved ro-vibrational transitions, or an unresolved vibrational

✉ Fax: +31-50-3634738, E-mail: e.r.t.kerstel@rug.nl

[1] Precision expressed in the so-called delta-notation (see (1)).

band) can be related directly to the abundance of the absorbing species, recording the spectrum containing abundant and rare isotopologue features, in both an unknown sample and an isotopically well-known reference material, enables one to relate the isotopic composition of the sample to that of the reference material in a manner as described in, e.g., [1]. Generally, the registration of the absorption signals is achieved by tuning the laser frequency in a (semi-)continuous manner over the spectral range of interest. In an alternative measurement scheme (at least) two different lasers are locked to the center-line frequencies of the abundant and rare isotopologue absorption features [7].

The relative deviation ${}^{x}\delta_{\mathrm{r}}(s)$ of the isotopic ratio of the sample (${}^{x}R_{\mathrm{s}}$), with respect to that of the reference (${}^{x}R_{\mathrm{r}}$) is given by:

$$ {}^{x}\delta_{\mathrm{r}}(s) \equiv \frac{{}^{x}R_{\mathrm{s}}}{{}^{x}R_{\mathrm{r}}} - 1 = \frac{({}^{x}n/{}^{a}n)_{\mathrm{s}}}{({}^{x}n/{}^{a}n)_{\mathrm{r}}} - 1 \,. \tag{1} $$

The subscript "s" refers to the sample, "r" to the reference material. The superscripts a and x refer to the most abundant (e.g., $^{12}C^{16}O_2$) and the rare isotope species (e.g., $^{13}C^{16}O_2$), respectively. With a proper choice of experimental conditions, the δ-value follows directly from the intensities in the spectra:

$$ {}^{x}\delta_{\mathrm{r}}(s) = \frac{({}^{x}\alpha/{}^{a}\alpha)_{\mathrm{s}}}{({}^{x}\alpha/{}^{a}\alpha)_{\mathrm{r}}} - 1 \,. \tag{2} $$

Here, $\alpha = \alpha(\nu_0) = Sf(\nu_0)n$ represents the experimentally determined (maximum) absorption coefficient at center-line frequency, provided that the line shape, given by the normalized line shape function f, is the same for all transitions. If not, one has to use the integrated line intensity (which, obviously, requires that the line profiles are determined over a sufficiently large spectral range). In (2) the (normally justified) assumption has been made that the (effective) optical path length l is the same for each isotopic species, or for the sample and reference spectra, or for both.

Since the line strength S depends on the number of molecules in the lower level of the transition, it is in general temperature-dependent (see, for example, [1]). Sample and reference spectra should therefore be measured at exactly the same temperature, and/or the isotopologue lines should be chosen such that their temperature coefficients are nearly equal. However, since to good approximation the measurement does not depend on the absolute temperature, but rather the difference between the sample and reference gas cells, passive stabilization with a good thermal contact between both gas cells is in most cases sufficient. With typical temperature coefficients for H_2O and CO_2 isotopologue lines in the range of (-5)–$(+5)$‰ K^{-1}, a differential temperature stability of 10 mK suffices to keep the temperature induced error below 0.1‰. Long-term absolute temperature stability is, however, important for measurement schemes that measure the sample and reference spectra not simultaneously but rather sequentially (in the same gas cell).

A careful selection of the spectral features is also important to assure that no interference from other species (whether other isotopologues or entirely different molecules) is present, while a similar absorption of the different isotopologues is desired in order to assure a comparable signal-to-noise ratio on all spectral lines of interest, and eventually the best precision on the isotope ratio determination. This is generally achieved by searching for a set of lines with similar absorption coefficients (taking into account the natural abundances of the isotopologues). The alternative of compensating a lower absorption coefficient (usually for the rare isotopologue) with a correspondingly longer optical path length has been used first, to the best of our knowledge, in [7], and was explored extensively for CO_2 in [8, 9].

The search for the best spectral region is further complicated by the requirement that all isotopologue lines, including at least one belonging to the major isotopologue and one to (one of) the rare isotopologue(s), occur within a narrow wavelength range, limited by the tuning range of the laser. In fact, the simultaneous measurements of the three major isotopic ratios in water ($\delta^{18}O$, $\delta^{17}O$, and $\delta^{2}H$) was demonstrated to be possible, in both the fundamental band near 2.73 μm [10] and the overtone band near 1.39 μm [11], thanks to the fortuitous occurrence of suitable ro-vibrational lines of the $H^{16}OH$, $H^{17}OH$, $H^{18}OH$, and $HO^{2}H$ isotopologues within a single laser frequency scan of about 1 cm^{-1} wide. In both spectral regions, very few other possibilities exist. This situation can be improved by the use of two lasers, each tuned to a different set of isotopologue lines [7, 12]. Whereas Uehara and colleagues [7] lock the two lasers to the peak of the absorption features of the rare and abundant isotopologues, in the scheme proposed by Gianfrani and colleagues [12], the two lasers are tuned over the respective absorptions, while being wavelength modulated at different, incommensurate frequencies. The two corresponding absorption spectra are retrieved from the detector signal using for each gas cell channel two phase-sensitive detectors, one for each modulation frequency. An alternative to this dual-wavelength multiplexing technique would be to time-division multiplex the signals from each gas cell, resulting in a slightly less complex setup, but at the cost of an increased measurement time.

3 Selected applications

3.1 *Applications of carbon dioxide and water isotope measurements*

As mentioned in the introduction, this paper focuses on laser-based isotope ratio measurements on carbon dioxide and water. Both are also highly relevant to the environment. Carbon dioxide is recognized as the principal anthropogenic driver of climate change, even though it is considered a trace gas in the Earth's atmosphere. In fact, its strong opacity in the infrared spectral region has a big impact on the environment, and is the principal component of the manmade contributions to the greenhouse effect. Analyses of the $^{13}CO_2/^{12}CO_2$ ratio, in conjunction with CO_2 concentration measurements, place important constraints on the global budget of atmospheric CO_2. Apart from the use in atmospheric research, $\delta^{13}CO_2$ finds many other relevant applications in several research fields, including soil science and ecology, plant and animal biology, geochemistry and vulcanology. In geochemical investigations of volcanic emissions, the $\delta^{13}CO_2$ parameter enables researchers to understand source-region changes, which are fundamental to monitor and forecast volcanic activity [13]. *Helicobacter pylori*

infections can be diagnosed in a non-invasive way by $\delta^{13}CO_2$ analysis of a subject's breath, after the ingestion of ^{13}C-labeled urea [14]. Stable carbon isotopic methods have been successfully applied for decades in various studies in ecology. For instance, it is possible to investigate the CO_2 exchanges among the different compartments of the environment, as well as the aboveground and belowground respiratory processes, including plant respiration, and litter and soil organic matter decomposition [15, 16].

Similarly, oxygen isotope analyses in oxygen-bearing molecules play an important role in atmospheric research for a number of interesting applications in which ^{17}O and ^{18}O are used as natural tracers. The $^{18}O/^{16}O$ and $^{17}O/^{16}O$ isotope ratios in carbon dioxide, as well as in water, are good indicators of troposphere–stratosphere exchange [17–19].

Although CO_2 is the greenhouse gas most strongly affected by human activity, water vapor is the most important natural greenhouse gas. In the troposphere, water vapor is responsible for global movement of latent heat energy, and controls radiation and cooling rates through its effect on cloud coverage. In the stratosphere, water vapor affects both the production of odd-hydrogen and the formation of stratospheric clouds, which in turn modulate polar ozone destruction [20–23]. Understanding the process of dehydration of air entering the stratosphere through the tropical tropopause, the relative importance of large scale and convective transport processes, and the origin and microphysical properties of radiatively important thin cirrus clouds in the tropical tropopause layer, are among the key issues in atmospheric science. In situ measurement of the water isotopic composition is believed to be vital in addressing these [24–27]. Close to the surface, the isotopic composition of moisture is crucial in understanding the hydrological cycle and its link to the carbon cycle through the exchange of oxygen atoms in the ecosystem [15, 28]. Isotope measurements on precipitation, whether recent or old (stored in the form of compressed snow in polar ice caps), are highly relevant for (palaeo-)climate studies [29, 30]. Finally, we mention the use of water isotopes in biomedical energy expenditure (metabolism) and total body water determinations [31, 32].

3.2 *Implementations of isotope measurements at elevated concentration levels*

The methane isotope measurements carried out by Bergamaschi and colleagues in the early 90s, using a lead-salt laser spectrometer, arguably represent the first successful application of a laser-based isotope ratio analyzer in the environmental sciences [33]. Inspired by this early work, the group at the University of Groningen, using a color center laser at 2.7 μm [10] and later diode lasers near 1.4 μm [11], demonstrated that a sufficiently high level of precision, as well as accuracy, can be attained in the measurement of water isotope ratios to be able to apply the technique successfully to biomedical energy expenditure measurements [34–36], ice-core palaeoclimate reconstruction [37], and plant leaf evaporation studies [38]. In fact, for the deuterium isotope ratio (δ^2H), and at high isotopic enrichment levels also the oxygen isotope ratios ($\delta^{17}O$ and $\delta^{18}O$), the level of precision is comparable to or exceeds that of IRMS. In these studies, liquid water samples ranging in size from 1 to 10 μl were injected into 20-m optical path length multiple pass cells. The one order of magnitude lower transition strength of the transitions at 1.4 μm, compared to the situation at 2.7 μm, was easily compensated for by the use of sensitive wavelength modulation detection. In Fig. 1 we show the layout of a typical experiment. For a more detailed discussion of these laboratory instruments we refer the reader to [1, 4]. Comparable or better performance can now be obtained with commercial near-infrared, cavity-based absorption spectrometers [39–41]. Furthermore, with the recent availability of a new generation of long wavelength, lateral grating, distributed feedback (DFB) diode lasers based on GaSbAs semiconductor heterostructures, it has become interesting and practical to return to the 2.7 μm region. These lasers have operational characteristics that are very similar to those of their shorter wavelength counterparts, including room temperature single-mode operation and an output power level of several mW [42]. The use of such a laser in our dual multiple-pass gas cell spectrometer enables us to work with a much shorter absorption path length, and will eventually result in a more compact setup [43]. Others have adopted this laser technology to develop a compact spectrometer that may one day measure water isotopes in the lower Martian atmosphere [44].

Similarly, near-infrared laser absorption spectroscopy has been extensively used to measure the $^{13}C/^{12}C$ isotope abundance ratio in gas phase carbon dioxide. The spectral window around the wavelength of 2 μm is very attractive for two im-

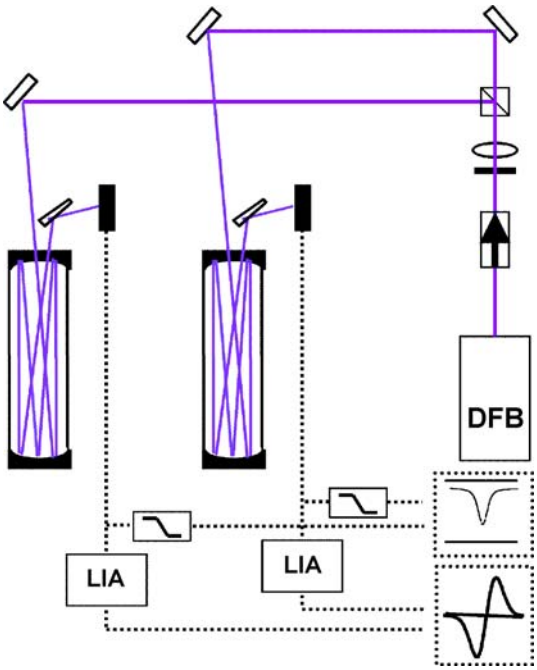

FIGURE 1 Layout of a typical dual gas cell, wavelength-modulation, diode laser spectrometer. DFB – distributed feedback diode laser, LIA – phase sensitive detector. The laser output passes an optical isolator before arriving at a 50% beam splitter. The sample and reference materials are held inside two identical multiple-reflection gas cells. The output is registered by two infrared detectors, of which the output signal is sent to a phase-sensitive detector for first or second harmonic signal recovery. A low pass filter permits the registration of the direct absorption signal (with the laser residual amplitude modulation removed)

portant reasons. First, it exhibits relatively strong $^{13}CO_2$ and $^{12}CO_2$ absorption features: Although three orders of magnitude weaker than the fundamental vibration at 4.3 μm, it is still two orders of magnitude stronger than the band in the telecom region at 1.6 μm. Several pairs of ro-vibrational lines show good properties for isotope ratio measurements in terms of spectral overlap, absorption intensity and temperature sensitivity [45]. Secondly, high quality, room temperature, DFB diode lasers are commercially available in this region. Implementing wavelength modulation spectroscopy to sensitively monitor the laser absorption in a multiple reflection cell, the feasibility of high precision $\delta^{13}C$ determinations in a 2% CO_2/N_2 mixture, representative of exhaled breath, was demonstrated [46].

Subsequently, a simplified implementation of this methodology, in which a single detector and associated electronics were used to probe absorptions from a pair of $^{13}CO_2$ and $^{12}CO_2$ lines, simultaneously in a sample and a reference single-pass cell, revealed great potential for in-situ $\delta^{13}CO_2$ determinations. Installed inside the crater of the Solfatara volcano (near Naples, Italy), the laser spectrometer was able to operate in a very harsh environment, providing isotope ratio data, back-traceable to the international standard material, with a precision and accuracy of 0.5‰ [47]. Examples of field determinations of the $^{13}CO_2/^{12}CO_2$ ratio are reported in Fig. 2, where the results of 10 repeated measurements are displayed for volcanic gases, properly sampled using either

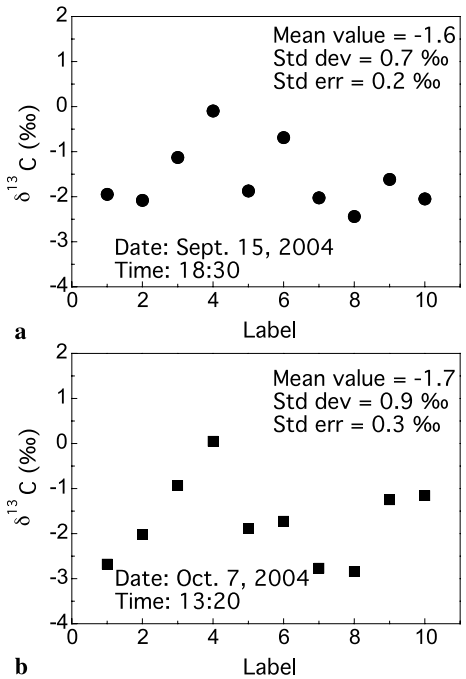

FIGURE 2 Examples of in situ measurements of the $^{13}C/^{12}C$ isotope ratio in CO_2, by means of a diode-laser based spectrometer, installed inside the crater of a volcano near Naples. The volcanic gas was sampled by means of an off-line, flask-based method (**a**), and a direct collection system (**b**). In the latter case, after being sampled through a homemade gas dryer and cooler, the volcanic gas was directly conveyed to the sample cell, thus ensuring a $\delta^{13}C$-monitoring in a quasi-continuous way. Each point is the result of a non-linear least squares analysis of a pair of sample and reference spectra. The overall acquisition time was about 83 and 50 min, respectively, for the measurement sets of (**a**) and (**b**)

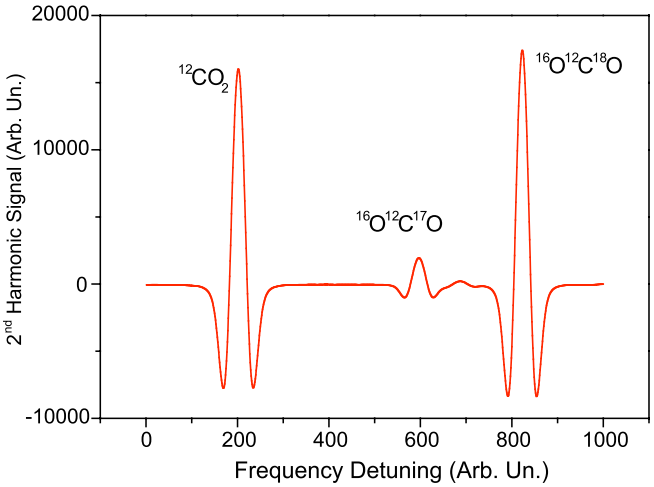

FIGURE 3 Example of a WMS spectrum near 2311.8 cm^{-1}, in a mixture 2% CO_2 in N_2, at a pressure of 35 Torr. The spectrum shows the $^{12}C^{16}O_2$ $P(15)$ transition belonging to the $2\nu_2^2+\nu_3-2\nu_2^2$ band, and the $^{16}O^{12}C^{17}O$ $P(33)$ and $^{16}O^{12}C^{18}O$ $P(25)$ transitions, both belonging to the ν_3 band

off-line or on-line methods, based on a homemade gas dryer and cooler. Thus, for the first time, continuous observations of the carbon isotopes in volcanic gases, which are of great importance for geochemical surveillance of volcanoes, became possible.

By virtue of the much elevated absorption strength of carbon dioxide, the spectral region around 4.3 μm enables the accurate measurement of $\delta^{13}CO_2$ in natural air samples. It also offers unique possibilities for simultaneous determinations of the $^{18}O/^{16}O$ and $^{17}O/^{16}O$ isotope ratios in atmospheric CO_2. Recently, a continuous-wave (cw), liquid-nitrogen cooled, distributed feedback quantum cascade laser (QCL) was used to probe $^{12}C^{16}O_2$, $^{16}O^{12}C^{18}O$, and $^{16}O^{12}C^{17}O$ lines near 2311.8 cm^{-1} (see Fig. 3) [48]. These isotope ratio measurements were carried out in a mixture of 2% CO_2 in N_2. The absorption path length in the single-pass gas cells of the wavelength modulated spectrometer amounted to just 25 cm. Increasing the path length to a still modest value of a few meters in a multiple-pass setup, would result in a robust, compact, and sensitive spectrometer for atmospheric studies.

3.3 *Isotope ratio measurements at trace level concentrations*

In the experiments we have considered so far, the concentration of the sample is not the limiting factor when considering the attainable precision. Rather, what is important is a very high signal-to-noise ratio, combined with an excellent instrument stability on a time scale comparable to the (re-) calibration of the isotope ratio measurement. Ultimately then, the measurements are limited by sample handling and sample introduction errors, but in practice many infrared instruments are limited by optical fringes.

There is, however, a growing interest in using optical instruments in applications in which the concentration of the sample is very low, most notably in situ isotopic analyses of atmospheric trace gases. Assuming that a further reduction of the noise level is not practically feasible, the use of either stronger transitions, or a longer effective optical

path length can still increase the sensitivity of the absorption measurement.

3.3.1 Taking advantage of mid-infrared absorption strengths. The first option requires that one moves from the near-infrared, overtone and combination band region to the mid-infrared, in order to excite stronger fundamental vibrations. This is particularly effective for molecules that exhibit strongly harmonic vibrations like CO_2, as we showed in the previous section. Since X−H (X=C, N, O, ...) oscillators are more anharmonic, the intensity difference between fundamental and overtone transitions is much less pronounced in the case of a molecule like water: the 2.7-μm fundamental stretching mode is only about one order of magnitude stronger than the band at 1.4 μm, while the bending mode near 7 μm is not much stronger than the 2.7-μm band. Thus, Bowling and co-workers put wavelength modulation of the 4.3-μm emission of a lead-salt diode laser to effective use in ecosystem-atmosphere exchange studies involving the measurement of the $^{13}CO_2/^{12}CO_2$ ratio [49]. In order to get away from the use of cryogenics, pulsed operation of a QCL in the same spectral region has been pioneered by McManus and colleagues at Aerodyne Research [50], as well as by Tittel and co-workers [51, 52]. Nelson and co-workers recently reported good results on $\delta^{13}CO_2$ and $\delta^{18}OCO$ measurements in atmospheric carbon dioxide, using a room-temperature QCL at 4.33 μm in combination with dual multiple-pass gas cells (reference and sample), and a novel spectral ratio data analysis method [53].

Non-cryogenic operation in the mid-infrared region can also be achieved through difference frequency generation (DFG), mixing the output of two high-quality near infrared lasers in a non-linear crystal. Although characterized by an excellent beam quality (desirable in order to suppress optical fringes in multiple-pass systems and to achieve good mode-matching in cw-CRDS setups) and good spectral coverage, such lasers have long suffered from very low output powers and high complexity (read: cost). Progress in near-infrared diode lasers, fiber technology, and the use of waveguides to increase the conversion efficiency, have assured that DFG lasers are still an important alternative to QCLs [54, 55].

3.3.2 Using optical cavities to increase the effective absorption path length. Increasing the optical path length, the second option, can be done very effectively through the use of a high finesse resonant optical cavity, in techniques like cavity ring down spectroscopy (CRDS) and cavity enhanced absorption spectroscopy (CEAS) [56, 57]. Compared to the commonly used multiple-pass cells, optical cavities offer the advantage of a 100–1000 times greater absorption path length, typically obtained in an equally smaller volume (with the prominent exception of off-axis CEAS – see below). In fact, in the presence of an absorbing medium, but in the thin sample regime, the absorption path length is enhanced with respect to the cavity length by a factor $2F/\pi$, F being the empty cavity finesse [59].

A fundamental problem with these techniques is that the higher the finesse, the narrower the transmission mode envelope of the cavity, and the more difficult it becomes to inject light into the cavity. This is particularly true for a cavity enhanced technique like off-axis cavity enhanced absorption spectroscopy (OA-CEAS), also known as off-axis integrated cavity output spectroscopy (OA-ICOS).[2] In OA-CEAS, the light throughput is reduced by a factor $2/(1-R)$, the same factor as associated with the absorption path length enhancement, but additionally by the practical inability to capture all of the light intensity at the exit of the relatively large diameter cavity (see, e.g., [58]). The large size of the cavity also increases the pumping requirements if a fast gas exchange is desired.

A possible solution to this light injection problem involves the use of a fast electronic feedback loop to lock the laser emission frequency to the transmission peak of the cavity, which is now generally used on-axis [40, 59, 60]. A tight lock is needed to produce a stable transmitted power, since the cavity acts as a sharp frequency discriminator, converting residual laser frequency noise into amplitude noise on the cavity transmission. This is particularly problematic in the case of CEAS, which, unlike CRDS, is sensitive to laser power noise. In other words, the bandwidth of the feedback loop must be as large as possible, with an optimum phase delay between error and correction signals [61].

The use of cw-CRDS alleviates this problem, and can yield a robust system, as demonstrated by the commercial spectrometers developed by Picarro Inc. [40].

Romanini and co-workers have advanced a different, but very elegant solution that involves the self-locking of the laser, due to feedback to the laser of the field present in the cavity. This approach has been shown to work with DFB diode lasers [62], as well as with extended cavity diode lasers [63]. The first isotope ratio measurements with this technique of optical feedback cavity enhanced spectroscopy (OF-CEAS) were done on water with an instrument designed to be flown on high-altitude aircraft [64]. It should deliver a better sensitivity than a traditional multi-pass arrangement, as used in the airborne Alias water isotope spectrometer of Webster and co-workers [65], by virtue of an about two orders of magnitude longer effective optical absorption path length. At the same time the gas cell volume is reduced by about the same factor (down to about 10 mL). This significantly reduces the flow rate needed to bring the gas exchange time, and therewith the memory-limited response time, down to an acceptable level (shorter than a few seconds). Ultimately, this reduces the weight (51 kg) and size of the instrument (< 50 l). Together with a low power consumption and the absence of cryogens, this makes it uniquely suited for operation on unmanned aerial vehicles and high altitude platforms. It flew on both the NASA DC-8 research aircraft and the stratospheric WB-57F. In the summer of 2006 it participated in the African Monsoon Multidisciplinary Analysis (AMMA) campaign on board the European M55 Geophysica stratospheric airplane, out of Ouagadougou, Burkina Faso [66]. Its laboratory precision at a water volume mixing ratio of 40 ppm is between 5‰ (for $\delta^{18}O$) and 50‰ ($\delta^{2}H$) with a 50 s averaging time. Due to a temperature control problem, the effective averag-

[2] We prefer to use the term cavity enhanced absorption spectroscopy (CEAS), since the acronym ICOS is also used for the Integrated Carbon Observatory System, a new European research infrastructure with the aim of quantifying and understanding the greenhouse gas balance of the European continent and of adjacent regions (http://icos-infrastructure.ipsl.jussieu.fr/).

ing time during the Geophysica deployment was limited to about 1 s, with a corresponding penalty for the measurement precision.

Essentially the same device was used to analyze near-surface atmospheric moisture, sampled from just outside the Groningen laboratory. In this case, instrumental precision ranges from 0.15‰ (δ^{18}O) to 1.3‰ (δ^{2}H) for a 20 s averaging time for water mixing ratios of 2500 ppm and above (see Fig. 4). Using a commercial (Campbell Scientific) liquid-nitrogen cooled, lead-salt diode laser spectrometer, Lee et al. obtained the same level of precision on δ^{18}O of ambient air (New Haven, CT), albeit with an averaging time of 1 h [67].

We are aware of only one other water isotope ratio spectrometer that has been flown on a high altitude aircraft. In order to obtain the highest possible precision of water isotope ratio measurements in the stratosphere by means of an in-situ instrument, the Anderson group at Harvard selected again a derivative of CRDS, in this case off-axis cavity enhanced absorption spectroscopy (OA-CEAS) [58, 68]. But instead of working in the near-infrared region, a cryogenically cooled mid-infrared quantum cascade laser was used to excite transitions in the 6.7 μm region. However, the one order of magnitude gain in sensitivity compared to the near-infrared comes at a cost: In order to suppress spurious noise, large diameter (4″) mirrors had to be used, significantly increasing the size of the optical cavity and the overall instrument, as well as its power consumption.

The high sensitivity of the OF-CEAS approach is presently being exploited also for the accurate determination of the $^{13}C/^{12}C$ isotope ratio in atmospheric carbon dioxide [69].

Perhaps the ultimate in spectroscopic, trace gas level, isotope ratio measurements is represented by recent efforts to measure $^{14}CO_2$ at natural abundance ($\sim 10^{-12}$), both presented at the SIRIS 2007 meeting. Cancio Pastor reported on the use of a frequency-comb referenced difference frequency generation laser in combination with cavity ring down spectroscopy to achieve a detection limit of $\sim 8 \times 10^{-11}$ in a 1 s bandwidth [70]. Murnick, using intra-cavity optogalvanic detection, reported a projected detection limit of better than 10^{-12} on microgram CO_2 samples and a few minutes averaging, making the method a viable alternative to accelerator mass spectrometry, for example for biomedical ^{14}C-tracer experiments [71, 72].

4 Calibration of isotope ratio measurements

The precision (repeatability) of isotope ratio measurements is determined by optical and electronic noise inherent to the experimental setup, as well as by (uncorrected variations in the) environmental parameters (such as temperature, pressure, or vibrations) that affect either the instrument, or the sample density, or both. A good way to visualize the precision of the instrument is to graph the Allan variance, or its square root, against the total measurement time [73, 74]. If this is done for the isotope determination on one given sample, the resulting "Allan plot" will reveal the stability time of the spectrometer (obviously, especially in the case of a continuous, on-line measurement, care should be taken that the concentration and composition of the sample do not change). Most optical spectrometers will initially show an

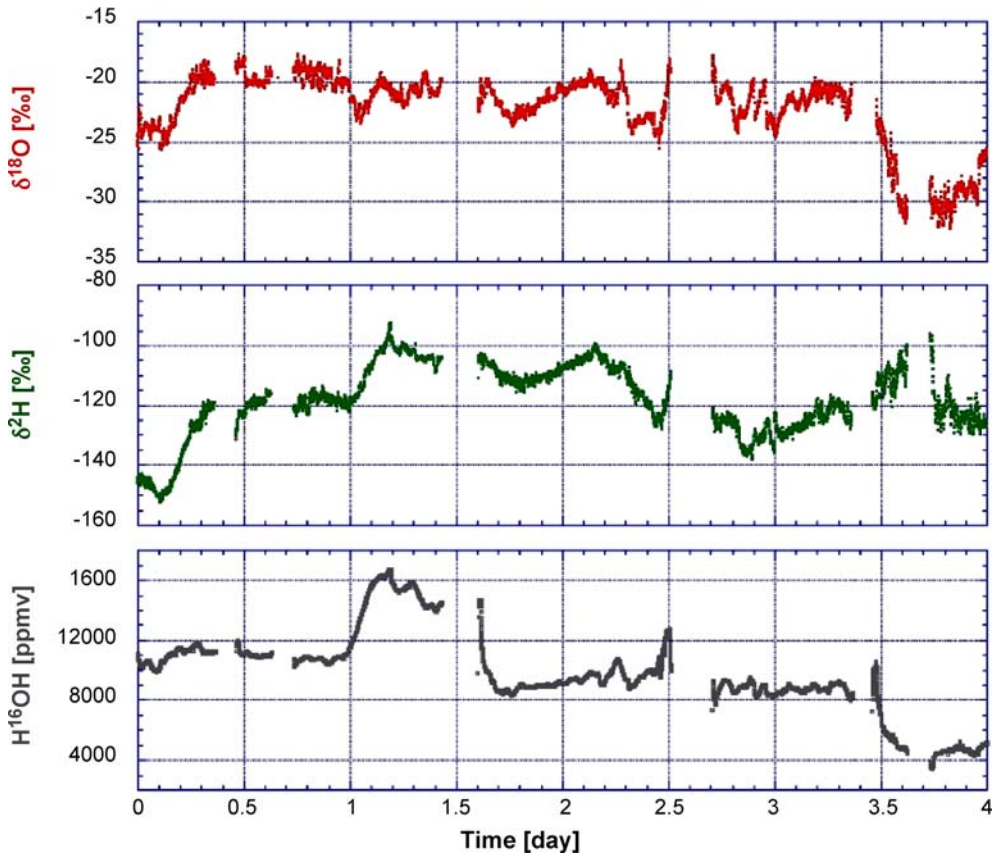

FIGURE 4 Continuous series of air moisture isotope measurements with a 15-s time resolution. The measurements were only interrupted for calibration measurements (not shown). The air was sampled from just outside the Groningen laboratory on four consecutive days in January 2006. One rain and two snow events can be identified in the data

Allan variance proportional to the reciprocal of the integration time, typical of white, random, uncorrelated noise, up to an optimum integration time, beyond which drift starts to dominate. The optimum integration time is often found to be in the range of 10 to several 100 s. If carried out in the above-described manner, the precision of the spectrometer may be reported as the square root of the Allan variance for a given integration time. This precision will, however, not include effects associated with the sample introduction (sample injection and subsequent incomplete evacuation of the gas cell, leading to memory effects) in a setup that operates in batch-mode. For this reason, we have more often reported the standard deviation of a series of repeated measurements, as a function of the total measurement time or number of averaged measurements, including re-introduction of a fresh sample of the same isotopic composition before each measurement.

In any case, ultimately more important than the precision is the measurement accuracy (trueness). We define the accuracy of the isotope ratio measurement as the root mean square of the difference between the calibrated (i.e., the corrected) measurements and the "true" values of a series of samples with known isotopic composition. These samples could be international standard materials as distributed by the International Atomic Energy Agency (IAEA), or local reference materials with their isotopic ratios determined by repeated mass spectrometric determinations. In what follows we discuss the calibration procedure and the data analysis that precedes it.

An advantage of the optical isotope ratio measurement is its conceptual simplicity: the ability to quantitatively understand the optical detection (Lambert–Beer) in great detail. This is a very fortunate situation compared to isotope ratio mass spectrometry, as the processes inside the ionization source of the mass spectrometer cannot be quantitatively understood at the same level of detail. Therefore, ideally, the calculation of the isotope signals takes as much experimental detail into account as possible. That is, the raw isotope ratio results ("delta-values") are corrected for all experimental imperfections that are theoretically and quantitatively understood. The thus corrected results are then calibrated on an internationally agreed upon isotope scale. For water the standard procedure calls for an absolute reference to the Vienna standard mean ocean water (VSMOW) international standard material and a linear stretching of the delta-scale, such that the measured values of VSMOW and standard light Antarctic precipitation (SLAP) match the internationally accepted values [75, 76]. A similar procedure is used for CO_2 [77–79]. The above is nicely demonstrated by the calibration procedure described by [10]: The practical difficulty of determining the true area under the measured absorption curves, due to spectral overlap and the recording of only a limited (and uncertain) spectral range, was circumvented by implementation of a data analysis procedure in which the isotope ratios ("δ-values") are retrieved by means of a line-by-line non-linear least-squares fit of the sample spectrum to the sum of the reference spectrum and a quadratic baseline, with a scaling parameter proportional to the ratio of the molecular densities of the corresponding isotopologues. The non-linear baseline is included to be able to account for wavelength dependence in the optic that splits the laser beam into the reference and sample beams, as well as for (stationary) slow etalon fringes in the optical system. This procedure, however convenient, introduces a dependence of the calculated delta-value on the pressure difference between the sample and gas cell. The resulting apparent shift in isotope ratio is an artifact of the data analysis procedure. It was experimentally measured, enabling the correction of the raw delta-values, and was shown to be in excellent agreement with computer model simulations [10].

The same data analysis procedure can also be used in experiments based on wavelength modulation spectroscopy (WMS) if one realizes that this procedure can be applied in the small absorption regime, assuring that the Fourier coefficients of the absorption profile are proportional to the species concentration associated with each spectral feature [11, 46]. In WMS-based isotope ratio spectrometry, an alternative spectral analysis procedure can be used, also in the "large absorption" regime, exploiting the formalism of the Fourier expansion of the harmonic signals. In fact, in the case of a second-harmonic detection scheme, an efficient approximation for the reconstruction and fitting of second-harmonic, wavelength-modulated, absorption spectra has been recently proposed and implemented [80]. The starting point was the work by Axner and co-workers [81, 82], but in our approach the Fourier analysis of WMS signals was combined with an analytical approximation to the Voigt line shape. It was shown to be highly accurate for trace gas concentration measurements and very significantly faster, and is likely to be extended to pairs of sample and reference spectra for retrieval of isotope ratios.

Other sources of systematic errors in the isotope ratio measurement include: 1) non-equal optical absorption path lengths associated with the reference and sample spectra; 2) a different chemical composition between sample and reference materials, and 3) detector non-linearity. The first effect plays a role only in the non-linear ("large absorption") regime of the Lambert–Beer law. Both the first and the second effect can be corrected for very precisely, in the case of a direct detection scheme, as demonstrated elsewhere [46, 83]. In the case of WMS detection, the calculation of the apparent isotope ratio shift, even though far from being trivial, is still possible by means of model simulations mentioned above. In WMS experiments, based on diode or quantum cascade lasers, a further source of systematic deviations comes from a small non-linear component in the detector responsitivity. Particularly when a large frequency separation occurs between the pair of isotopologue lines under investigation, the laser source must undergo a wide excursion of the injection current in order to enter into resonance with the two lines within a single frequency scan. This may translate into a significant power variation. As a consequence, the responsitivity of the signal and reference detectors may change slightly when the laser frequency moves from one absorption line to the other, the two variations not being necessarily equal. This effect can introduce an apparent shift in the measured isotope ratio.

It is possible to derive a theoretical formula to quantify the systematic error described above, under the assumption of (WMS) signals proportional to the fractional absorption, in the limit of identical temperatures and total pressures in the two cells [84]. According to (1), the measured δ-value is given

by:

$$\delta^x A_{\text{measured}} = \frac{{}^x W_\text{s}/{}^x W_\text{r}}{{}^a W_\text{s}/{}^a W_\text{r}} - 1\,, \tag{3}$$

where W is the WMS signal, the subscripts "r" and "s" refer to the reference and sample gases, while the superscripts "x" and "a" refer to the rare and most abundant isotopic species, respectively, and A represents the chemical species of interest. If Δ denotes the center line fractional absorption, P the laser power, and ϱ the detector responsitivity, the δ-value can be rewritten in this way:

$$\delta^x A_{\text{measured}} = \frac{\frac{\varrho_\text{s}(T^x P_\text{s})^x \Delta_\text{s}{}^x P_\text{s}}{\varrho_\text{r}(T^x P_\text{r})^x \Delta_\text{r}{}^x P_\text{r}}}{\frac{\varrho_\text{s}(T^a P_\text{s})^a \Delta_\text{s}{}^a P_\text{s}}{\varrho_\text{r}(T^a P_\text{r})^a \Delta_\text{r}{}^a P_\text{r}}} - 1\,, \tag{4}$$

with T the zero-pressure transmission of each cell, determined by the mirror reflectivity and by the number of reflections. Equation (4) takes into account the fact that the laser beams shining on the two cells may be of different power, which is determined by the reflectivity R_BS of the beam splitter dividing the primary beam into the two parts, as well as the fact that two detectors may exhibit a different responsitivity, ϱ_s and ϱ_r, for the sample and reference channels respectively. In particular for mid-infrared photoconductive detectors, the responsitivity ϱ may be a function of the laser power impinging on the detector. Not surprisingly, the larger the difference in the non-linear behavior of the detectors, the larger the error. But a less intuitive result is that, even if the two detectors exhibit the same non-linearity (or a single detector scheme is adopted), a systematic measurement error is made if the reference and signal detector (beams) do not receive the same level of optical power.

Standard InGaAs detectors are extremely linear, and this effect can be safely ignored in the near infrared region at wavelengths shorter than say 1.7 μm. However, extended-InGaAs detectors exhibit an appreciable non-linearity, as do all common mid-infrared detectors, and the described effect can be observed. Depending on the power levels and the degree of detector non-linearity, the apparent delta-shift can range from −2 to +2‰, in the case of an experiment at 2 μm using extended-InGaAs detectors [84].

In many cases, the systematic measurement errors mentioned above can be calibrated "away", through repeated measurements of reference materials, as long as the instrument is sufficiently precise and remains stable over time intervals larger than the time between calibration measurements. One should not, however, desire such a situation, as it makes the calibration process susceptible to unknown variations in environmental variables (pressure, temperature, laser power, etc.), and (often needlessly) complicated. For example, the correction terms determined in the calibration process may also show a dependence on the actual isotope ratio value, besides the dependence on the environmental variable. It is for these reasons that we prefer to correct the raw measurement results for experimental artifacts, as long as these are quantitatively well understood, before calibrating the measurements, based on the measurement of reference materials that are back-traceable to international standard materials (such as SLAP and VSMOW in the case of water isotope ratio measurements).

5 Conclusions

Recent developments in the field of laser spectroscopy, most notably the availability of easier to use mid-infrared laser sources and robust ultra-sensitive, cavity-based detection techniques, have led to important advances in our ability to measure isotope ratios at low concentrations of the gas of interest, under difficult conditions, and on more difficult systems. We have shown examples of attempts to measure in the harsh environment of a volcano, as well as at trace gas concentration levels on airborne platforms. Measurements have already been carried out on molecular systems that can be considered more difficult in terms of spectroscopic complexity than, for example, carbon dioxide. If we ignore sample handling related difficulties (such as may be prominent in the case of "sticky" or reactive species), and do not consider the environment in which the measurement needs to be carried out (e.g., on a moving platform, high temperature variability, or in the presence of other, interfering species), we propose that the product of the concentration of the isotopic species and the band strength, divided by the partition function, is a measure of the spectroscopic "ease of measurement". The latter may be quantified by:

$$E = p\upsilon \frac{RS_\text{r}S_a}{RS_\text{r} + S_a}\,. \tag{5}$$

Here, p represents the total pressure of the sample, υ is the volume mixing ratio of the abundant isotopologue, R is the isotope ratio, S_r is the line strength of the spectral feature used to probe the rare isotopologue, while S_a is that of the abundant isotopologue (for which we assume $R_a = 1$). Note that a molecular spectroscopy database like HITRAN reports the product of R and S as the line strength [85]. The formula takes into account that the ease of measurement is predominantly determined by the spectral feature (corresponding to the rare or abundant isotopologue) with the lowest signal strength. Underlying assumptions are that the laser line width is narrow compared to the absorption line width, that the absorption path lengths associated with the rare and abundant spectral features are equal, and that the measurement is carried out at a total pressure sufficiently low for the line broadening to remain within the Doppler limit, as at higher pressure the center line intensity no longer increases approximately linearly with pressure and spectral line overlap may result in isotopologue cross-correlations. In Table 1 we list the calculated values of E for a number of molecular systems, and experimental conditions (pressure, volume mixing ratio, line selection) as encountered in selected publications. We also report the inverse of the relative value, E^*, with respect to the determination of δ^{18}O in 100% water vapor at 2.73 μm (which thus has $E^* = 1$).

Roughly speaking, when the value of $1/E^*$ does not exceed 1000, a precise measurement can be carried out without the need to resort to very long optical path length, cavity enhanced techniques. Long path length multiple-pass cells can be rather susceptible to sinusoidal modulations of the spectrum baseline (fringes), induced by partial overlap of beam paths inside the cell. High finesse optical cavity based techniques too can suffer from unwanted reflections in the optical system, similarly leading to optical fringes, as well

Reference	Isotope	Wavelength [μm]	Total pressure [mbar]	υ [ppm]	RS_x [cm/molecule]	S_a [cm/molecule]	E [mbar ppm cm/molecule]	E^*	$1/E^*$
Kerstel et al.	$H^{18}OH$	1.39	36	1 000 000	6.2×10^{-24}	3.1×10^{-24}	7.4×10^{-17}	1.4×10^{-1}	7.0
2002 [11]	HOD	1.39	36	1 000 000	3.5×10^{-25}	3.1×10^{-24}	1.1×10^{-17}	2.2×10^{-2}	46.2
Kerstel et al.	$H^{18}OH$	2.73	36	1 000 000	1.8×10^{-23}	7.5×10^{-23}	5.2×10^{-16}	1	1
1999 [10]	HOD	2.73	36	1 000 000	1.2×10^{-23}	7.5×10^{-23}	3.7×10^{-16}	7.1×10^{-1}	1.4
Kerstel et al.	$H^{18}OH$	1.39	50	4	6.2×10^{-24}	3.1×10^{-24}	4.1×10^{-22}	7.9×10^{-7}	1.2×10^{6}
2006 [64]	HOD	1.39	50	4	3.5×10^{-25}	3.1×10^{-24}	6.3×10^{-23}	1.2×10^{-7}	8.3×10^{6}
Kerstel et al.	$H^{18}OH$	2.73	50	4	1.8×10^{-23}	7.5×10^{-23}	2.9×10^{-21}	5.6×10^{-6}	1.8×10^{5}
2008 (work in progress)	HOD	2.73	50	4	1.3×10^{-23}	7.5×10^{-23}	2.2×10^{-21}	4.2×10^{-6}	2.4×10^{5}
Gagliardi et al. 2003 [46]	$^{13}CO_2$	2.008	67	20 000	7.1×10^{-24}	2.1×10^{-24}	2.2×10^{-18}	4.2×10^{-3}	241
Castrillo et al. 2004 [47]	$^{13}CO_2$	2.008	18	980 000	7.1×10^{-24}	4.4×10^{-23}	1.1×10^{-16}	2.1×10^{-1}	4.8
Nelson et al.	$^{13}CO_2$	4.33	80	380	6.5×10^{-21}	4.7×10^{-21}	8.2×10^{-17}	1.6×10^{-1}	6.4
2008 [53]	^{18}OCO	4.33	80	380	4.6×10^{-21}	4.7×10^{-21}	7.1×10^{-17}	1.4×10^{-1}	7.4
Castrillo et al.	^{17}OCO	4.33	47	20 000	5.2×10^{-22}	4.6×10^{-21}	4.4×10^{-16}	8.5×10^{-1}	1.2
2007 [48]	^{18}OCO	4.33	47	20 000	5.2×10^{-21}	4.6×10^{-21}	2.3×10^{-15}	4.4	0.2
Waechter, Sigrist	$^{14}N^{15}NO$	4.57	50	825	3.4×10^{-21}	2.1×10^{-19}	1.4×10^{-16}	2.6×10^{-1}	3.8
2007 [86][a]	$^{15}N^{14}NO$	4.57	50	825	3.3×10^{-21}	2.1×10^{-19}	1.3×10^{-16}	2.5×10^{-1}	3.9
Halmer et al. 2005 [87][a]	^{15}NO	5.33	50	11	2.4×10^{-22}	1.7×10^{-22}	5.4×10^{-20}	1.0×10^{-4}	9.6×10^{3}

[a] Note that the mixing ratios used in these two studies ([86] and [87]) are a factor of, respectively, ~ 2600 and ~ 550 higher than natural.

TABLE 1 The "ease of measurement" parameter E for a number of selected molecular systems. The next to last column gives the parameter scaled to 1 for the reference measurement at 2.73 μm of $H^{18}OH$ in a 100% water vapor sample, while the final column gives the inverse of the relative parameter (thus increasing with the difficulty of the measurement). Note that the parameter does not account for the technique used to perform the measurement, nor does it relate to the success (precision, accuracy) of the experiment mentioned in the first column

as from unwanted feedback to the laser and laser phase noise. Short path length operation, using mid-infrared lasers if needed, may be preferable for these reasons alone. In addition, a multiple-pass cell is more easily used in a dual gas cell configuration, in which the sample spectrum can be recorded simultaneously with a reference spectrum. This will result in a partial cancelation of coherent (laser) noise when these spectra are compared (either by determining the ratio of absorptions, or the difference, as done in [54]). It also relaxes the stability requirements on the spectrometer, as the reference measurements will otherwise need to be interspersed at regular intervals (which should ideally be shorter than the Allan variance stability time of the spectrometer) between the sample measurements. It may be clear that these reference measurements do not eliminate the need for the frequent measurement of a number (minimum two) of standard materials that can be used for the isotope scale calibration as discussed in the previous section.

As the table shows, there are a (growing) number of applications that demand the utmost in detection sensitivity. Two promising techniques that can deliver such sensitivity are OA-CEAS and OF-CEAS. The first suffers from a low light throughput, and consequently requires a fairly high laser power and a good signal detection system. It also uses large diameter mirrors and therefore a large volume gas cell. This, in turn, results in a large pumping requirement, if the gas exchange time needs to be kept short. OF-CEAS shares the advantage of a very small cavity volume with cw-CRDS, but has the added advantage of a very high light transmission. However, OF-CEAS places specific requirements on the laser in terms of its sensitivity to optical feedback, excluding, for example, the use of a fibred DFG source. It is also the (slightly) more difficult technique to implement, due to the necessity to control the phase of the light field fed back to the laser, which is done by fine adjusting the distance between the laser and the cavity entrance mirror. The required bandwidth of this control loop (< 100 Hz) is, however, orders of magnitude lower than that required in conventional CEAS. As so often therefore, each technique presents its specific advantages and shortcomings, making the choice of technique highly dependent on the details of the application.

ACKNOWLEDGEMENTS We are indebted to past and present students and post-doctoral fellows who work(ed) in our laboratories, as well as our colleagues, including Gianluca Gagliardi, Daniele Romanini, Hans-Jürg Jost, and Harro Meijer. We thank two anonymous reviewers for their careful reading of, and useful comments on the manuscript.

REFERENCES

1 E.R.T. Kerstel, In: *Handbook of Stable Isotope Analytical Techniques*, ed. by P.A. de Groot (Elsevier, Amsterdam, 2004), Chapt. 34, pp. 759–787

2 C. Horita, J. Kendall, In: *Handbook of Stable Isotope Analytical Techniques*, ed. by P.A. de Groot (Elsevier, Amsterdam, 2004), Chapt. 1

3 W. Brand, In: *Handbook of Stable Isotope Analytical Techniques*, ed. by P.A. de Groot (Elsevier, Amsterdam, 2004), Chapt. 38
4 E.R.T. Kerstel, H.A.J. Meijer, In: *Isotopes in the Water Cycle: Past, Present and Future of a Developing Science*, ed. by P.K. Aggarwal, J. Gat, K. Froehlich, IAEA Hydrology Section (Springer, Dordrecht, 2005), pp. 109–124
5 W.A. Brand, H. Avak, R. Seedorf, D. Hofmann, T. Conradi, Isot. Environ. Health Stud. **32**, 263 (1996)
6 H.A.J. Meijer, In: New Approaches for Stable Isotope Ratio Measurements (Proc. of Advisory Group Meeting, 1999), IAEA-TECDOC-1247 (IAEA, Vienna, 2001), pp. 105–112
7 K. Uehara, K. Yamamoto, T. Kikugawa, N. Yoshida, Sens. Actuators B **74**, 173 (2001)
8 J.B. McManus, M.S. Zahniser, D.D. Nelson, L.R. Williams, C.E. Kolb, Spectrochim. Acta A **58**, 2465 (2002)
9 D. Weidmann, C.B. Roller, C. Oppenheimer, A. Fried, F.K. Tittel, Isot. Environ. Health Stud. **41**, 293 (2005)
10 E.R.T. Kerstel, R. van Trigt, N. Dam, J. Reuss, H.A.J. Meijer, Anal. Chem. **71**, 5297 (1999)
11 E.R.T. Kerstel, G. Gagliardi, L. Gianfrani, H.A.J. Meijer, R. van Trigt, R. Ramaker, Spectrochim. Acta A **58**, 2389 (2002)
12 L. Gianfrani, G. Gagliardi, M. van Burgel, E.R.T. Kerstel, Opt. Express **11**, 1566 (2003)
13 G. Capasso, M. Carapezza, C. Federico, S. Inguaggiato, A. Rizzo, Bull. Volcanol. **68**, 118 (2005)
14 V. Savarino, S. Vigneri, G. Celle, Gut **45**, 18 (1999)
15 D. Yakir, L.S.L. Sternberg, Oecologia **123**, 297 (2000)
16 S. Trumbore, Global Change Biol. **12**, 141 (2006)
17 A. Zahn, P. Franz, C. Bechtel, J.U. Grooss, T. Rockmann, Atmos. Chem. Phys. **6**, 2073 (2006)
18 R. Shaheen, C. Janssen, T. Rockmann, Atmos. Chem. Phys. **7**, 495 (2007)
19 M.C. Liang, G.A. Blake, B.R. Lewis, Y.L. Yung, Proc. Nat. Acad. Sci. USA **104**, 21 (2007)
20 J.E. Harries, Q. J. R. Meteorol. Soc. **123**, 2173 (1997)
21 P.M.D. Forster, K.P. Shine, Geophys. Res. Lett. **29**, 4 (2002)
22 D.B. Kirk-Davidoff, E.J. Hintsa, J.G. Anderson, D.W. Keith, Nature **402**, 399 (1999)
23 D.B. Kirk-Davidoff, D.P. Schrag, J.G. Anderson, Geophys. Res. Lett. **29**, 4 (2002)
24 E.J. Moyer, F.W. Irion, Y.L. Yung, M.R. Gunson, Geophys. Res. Lett. **23**, 2385 (1996)
25 D.W. Keith, J. Geophys. Res. **105**, 15 167 (2000)
26 G.A. Schmidt, G. Hoffmann, D.T. Shindell, Y. Hu, J. Geophys. Res. D **110**, 21 314 (2005)
27 B. Toon, E. Jensen, J. Holton, J. Logan, P. Newman, R.J. Salawitch, D. Starr, D. Waugh, P.O. Wennberg, Draft of Tropical Composition, Cloud and Climate Coupling Experiment (TC4) (NASA Goddard Space Flight Center, MD, 2003), http://www.espo.nasa.gov/tc4/science.php
28 X.F. Wang, D. Yakir, Hydrol. Proc. **14**, 1407 (2000)
29 W. Dansgaard, Tellus **16**, 436 (1964)
30 J. Jouzel, R.B. Alley, K.M. Cuffey, W. Dansgaard, P. Grootes, G. Hoffmann, S.J. Johnsen, R.D. Koster, D. Peel, C.A. Shuman, M. Stievenard, M. Stuiver, J.J. White, Geophys. Res. **102**, 26 471 (1997)
31 J.R. Speakman, *Doubly Labelled water: Theory and Practice* (Chapman and Hall, London, 1997)
32 J.R. Speakman, Isot. Environ. Health Stud. **41**, 335 (2005)
33 P. Bergamaschi, M. Schupp, G.W. Harris, Appl. Opt. **33**, 7704 (1994)
34 R. van Trigt, E.R.T. Kerstel, G.H. Visser, H.A.J. Meijer, Anal. Chem. **73**, 2445 (2001)
35 R. van Trigt, E.R.T. Kerstel, H.A.J. Meijer, M. McLean, G.H. Visser, J. Appl. Physiol. **93**, 2147 (2002)
36 E.R.T. Kerstel, T. Piersma, J. Gessaman, A. Dekinga, H.A.J. Meijer, H. Visser, Isot. Environ. Health Stud. **42**, 1 (2006)
37 R. van Trigt, H.A.J. Meijer, A.E. Sveinbjornsdottir, S.J. Johnsen, E.R.T. Kerstel, Ann. Glaciol. **35**, 125 (2002)
38 E.R.T. Kerstel, L.G. Van der Wel, H.A.J. Meijer, Isot. Environ. Health Stud. **41**, 207 (2005)
39 P. Aggarwal, M. Groening, M. Gupta, T. Owano, D. Baer, Laser spectroscopic analysis of stable isotopes in natural waters, Eos trans. AGU, 87(52), Fall Meeting Suppl., Abstract H51D-504 (2006)
40 E. Crosson, High accuracy isotopic measurements using CRDS, 2nd International Workshop on Stable Isotope Ratio Infrared Spectrometry (SIRIS 2007), Sept. 7–8, 2007, Firenze, Italy
41 G. Lis, L.I. Wassenaar, M.J. Hendry, Anal. Chem. **80**, 287 (2008)
42 http://www.nanoplus.com/, Accessed 1 July 2008
43 V. Gkinis, E. Kerstel, Water isotope ratio measurements using a distributed feedback diode laser at 2730 nm, 2nd International Workshop on Stable Isotope Ratio Infrared Spectroscopy (SIRIS 2007), Sept. 2–7, 2007, Firenze, Italy
44 G. Durry, L. Joly, T. Le Barbu, B. Parvitte, V. Zeninari, Infrared Phys. Technol. **51**, 229 (2008)
45 G. Gagliardi, R. Restieri, G. Casa, L. Gianfrani, Opt. Laser Eng. **37**, 131 (2002)
46 G. Gagliardi, A. Castrillo, R.Q. Iannone, E. Kerstel, L. Gianfrani, Appl. Phys. B **77**, 119 (2003)
47 A. Castrillo, G. Casa, M. van Burgel, D. Tedesco, L. Gianfrani, Opt. Express **12**, 6515 (2004)
48 A. Castrillo, G. Casa, L. Gianfrani, Opt. Lett. **32**, 3047 (2007)
49 D.R. Bowling, S.D. Sargent, B.D. Tanner, J.R. Ehleringer, Agric. For. Meteorol. **118**, 1 (2003)
50 J.B. McManus, D.D. Nelson, J.H. Shorter, R. Jimenez, S. Herndon, S. Saleska, M. Zahniser, J. Mod. Opt. **52**, 2309 (2005)
51 D. Weidmann, F.K. Tittel, T. Aellen, M. Beck, D. Hofstetter, J. Faist, S. Blaser, Appl. Phys. B **79**, 907 (2004)
52 D. Weidmann, G. Wysocki, C. Oppenheimer, F.K. Tittel, Appl. Phys. B **80**, 255 (2005)
53 D.D. Nelson, J.B. McManus, M.S. Zahniser, B. Tuzson, L. Emmenegger, Appl. Phys. B **90**, 301 (2008)
54 D. Richter, P. Weibring, A. Fried, O. Tadanaga, Y. Nishida, M. Asobe, H. Suzuki, Opt. Express **15**, 564 (2007)
55 J.J. Scherer, Mid-infrared trace gas sensing with difference frequency generation lasers, International Conference on Field Laser Applications in Industry and Research (FLAIR 2007), Sept. 2–7, 2007, Firenze, Italy
56 G. Berden, P. Peeters, G. Meijer, Int. Rev. Chem. Phys. **19**, 565 (2000)
57 M. Mazurenka, A.J. Orr-Ewing, R. Peverall, G.A.D. Ritchie, Ann. Rep. Prog. Chem. C **101**, 100 (2005)
58 E.J. Moyer, D.S. Sayres, G.S. Engel, J.M. St. Clair, F.N. Keutsch, N.T. Allen, J.H. Kroll, J.G. Anderson, Appl. Phys. B, this issue (2008)
59 L. Gianfrani, R.W. Fox, L. Hollberg, J. Opt. Soc. Am. B **16**, 2247 (1999)
60 B. Paldus, C.C. Harb, T.G. Spence, B. EWilke, J. Xie, J.S. Harris, R.N. Zare, J. Appl. Phys. **83**, 3991 (1998)
61 G. Gagliardi, L. Gianfrani, Opt. Laser Eng. **37**, 509 (2002)
62 J. Morville, D. Romanini, A.A. Kachanov, M. Chenevier, Appl. Phys. B **78**, 465 (2004)
63 V. Motto-Ros, J. Morville, P. Rairoux, Appl. Phys. B **87**, 531 (2007)
64 E.R.T. Kerstel, R.Q. Iannone, M. Chenevier, S. Kassi, H.-J. Jost, D. Romanini, Appl. Phys. B **85**, 397 (2006)
65 C.R. Webster, A. Heymsfield, Science **302**, 1742 (2003)
66 F. Cairo, K. Law, H. Schlager, S. Balestri, C. Blom, S. Borrmann, J. Curtius, M. De Reus, F. Fierli, A. Garnier, E.R.T. Kerstel, P. Konopka, P. Mazzinghi, F. Olschewski, A. Oulanovsky, F. Ravegnani, C. Schiller, G. Shur, N. Sitnikov, M. Streibel, M. Stefanutti, F. Stroh, T. Roeckmann, S. Viciani, H. Voessing, C. Voigt, M. Volk, M. von Hobe, R. Weiger, V. Yushkov, Geophys. Res. Abstr. **9**, 06 899 (2007)
67 X. Lee, S. Sargent, R. Smith, B. Tanner, J. Atmos. Ocean Technol. **22**, 555 (2005)
68 T.F. Hanisco, E.J. Moyer, E.M. Weinstock, J.M.S. Clair, D.S. Sayres, J.B. Smith, R. Lockwood, J.G. Anderson, A.E. Dessler, F.N. Keutsch, J.R. Spackman, W.G. Read, T.P. Bui, Geophys. Res. Lett. **34**, 5 (2007)
69 R. Wehr, S. Kassi, D. Romanini, L. Gianfrani, Appl. Phys. B, this issue (2008)
70 P. Cancio Pastor, Frequency comb assisted mid-infrared high-sensitivity spectroscopy, 2nd International Workshop on Stable Isotope Ratio Infrared Spectrometry (SIRIS 2007), Sept. 7–8, 2007, Firenze, Italy
71 D.E. Murnick, Intracavity optogalvanic spectroscopy (ICOGS): An ultra-sensitive technique for $^{14}CO_2$ detection, 2nd International Workshop on Stable Isotope Ratio Infrared Spectrometry (SIRIS 2007), Sept. 7–8, 2007, Firenze, Italy
72 D.E. Murnick, O. Dogru, E. Ilkmen, Nucl. Instrum. Methods B **259**, 786 (2007)
73 D.W. Allan, Proc. IEEE **54**, 221 (1966)
74 P. Werle, R. Mucke, F. Slemr, Appl. Phys. B **57**, 131 (1993)
75 R. Confiantini, Advisory Group meeting on stable isotope reference samples for geochemical and hydrological investigations. Report to the Director General, IAEA, Vienna 1984
76 G. Hut, Consultants' Group meeting on stable isotope reference samples for geochemical and hydrological investigations. IAEA report, Vienna 1986

77 T.B. Coplen, In: *Reference and Intercomparison Materials for Stable Isotopes of Light Elements*, IAEA-TECDOC-825 (IAEA, Vienna, 1995), pp. 31–34
78 C.E. Allison, R.J. Francey, H.A.J. Meijer, In: *Reference and Intercomparison Materials for Stable Isotopes of Light Elements*, IAEA-TECDOC-825 (IAEA, Vienna, 1995), pp. 155–162
79 M.F. Miller, T. Röckmann, I.P. Wright, Geochim. Cosmochim. Acta **71**, 3145 (2007)
80 E. De Tommasi, G. Casa, A. Castrillo, L. Gianfrani, J. Quant. Spectrosc. Radiat. Transf. **109**, 168 (2008)
81 O. Axner, P. Kluczynski, A.M. Lindberg, J. Quant. Spectrosc. Radiat. Transf. **68**, 299 (2001)
82 P. Kluczynski, J. Gustafsson, A.M. Lindberg, O. Axner, Spectrochim. Acta B **56**, 1277 (2001)
83 A. Castrillo, G. Casa, E. Kerstel, L. Gianfrani, Appl. Phys. B **81**, 863 (2005)
84 A. Castrillo, G. Casa, A. Palmieri, L. Gianfrani, Isot. Environ. Health Stud. **42**, 47 (2006)
85 L.S. Rothman, D. Jacquemart, A. Barbe, D.C. Benner, M. Birk, L.R. Brown, M.R. Carleer, C. Chackerian, K. Chance, L.H. Coudert, V. Dana, V.M. Devi, J.M. Flaud, R.R. Gamache, A. Goldman, J.M. Hartmann, K.W. Jucks, A.G. Maki, J.Y. Mandin, S.T. Massie, J. Orphal, A. Perrin, C.P. Rinsland, M.A.H. Smith, J. Tennyson, R.N. Tolchenov, R.A. Toth, J. Vander Auwera, P. Varanasi, G. Wagner, J. Quant. Spectrosc. Radiat. Transf. **96**, 139 (2005)
86 H. Waechter, M.W. Sigrist, Appl. Phys. B **87**, 539 (2007)
87 D. Halmer, G. Von Basum, M. Horstjann, P. Hering, M. Mürtz, Isot. Environ. Health Stud. **41**, 303 (2005)